# OPTICS DESIGN AND COLLIMATION EFFICIENCY OF THE FERMI@ELETTRA COLLIMATION SYSTEM

S. Di Mitri#, S. Ferry, Sincrotrone Trieste (ELETTRA), Trieste, Italy

*Abstract*

Horizontal scraping, geometric and energy collimation of the Fermi@elettra electron beam has been investigated analytically and with the *elegant* particle tracking code. Beam scraping in the first magnetic bunch length compressor has been characterized in terms of reduction of the transverse emittance and variation of the energy chirp induced by the succeeding linac longitudinal wake field. The locations of the geometric and energy collimators have been identified in the machine lattice. A novel definition of collimation efficiency is proposed that allowed us to identify a configuration of the collimation system that is a compromise between the collimation performance, optics design and available space.

## MOTIVATIONS

A Collimation System (CS) has been developed for the FERMI@elettra [1,2] linac based Free Electron Laser (FEL). Its final aims are: i) protect the undulators from the radiation damage (demagnetization) induced by spurious particles that may hit the low gap vacuum chamber; ii) manipulate the transverse and longitudinal profile of the electron beam. These goals will be accomplished by the CS: a) by stopping the dark current [3,4] generated in the RF structures; b) by removing the beam halo [5,6] generated by space charge at low energy and by geometric and chromatic aberrations, magnetic compression, transverse wake field, misteering and mismatching of the regular beam. While goal i) will be accomplished by the collimators properly-called, goal ii) will be achieved with movable scrapers located in dispersive regions of the FERMI lattice. In both cases i) and ii), suppression of the undesired particles will not affect the seeded FEL process as only electrons in the bunch core are expected to contribute to lasing.

## SCRAPERS

### *Optics*

Scrapers are blades moving in the bending (i.e. horizontal) plane. They are located in the inner drift of the magnetic bunch compressors (BC1 and BC2), where the dispersion has its maximum. Figure 1 shows the optics up to the BC1 area.

Optics mismatch induced by space charge in the injector and Coherent Synchrotron Radiation (CSR) [7] emitted in BC1 induce an energy mismatch of the bunch edges w.r.t. the core; thus, particle in the edges deviate appreciably from the nominal trajectory in the dispersive regions. Moreover, CSR enlarges the emittance at the edges because of the optics mismatch in this region. These two effects contribute to the emittance growth, as shown in Figure 2. The *elegant* code [8] was used to perform particle tracking and to model the scraper like an ideal absorber (no particle scattering).

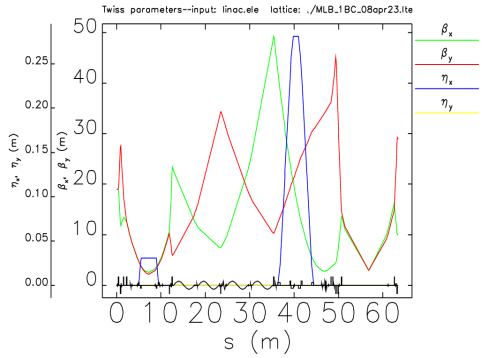


Figure 1: Twiss functions from the injector end (100MeV) to the BC1 diagnostic area (250MeV).

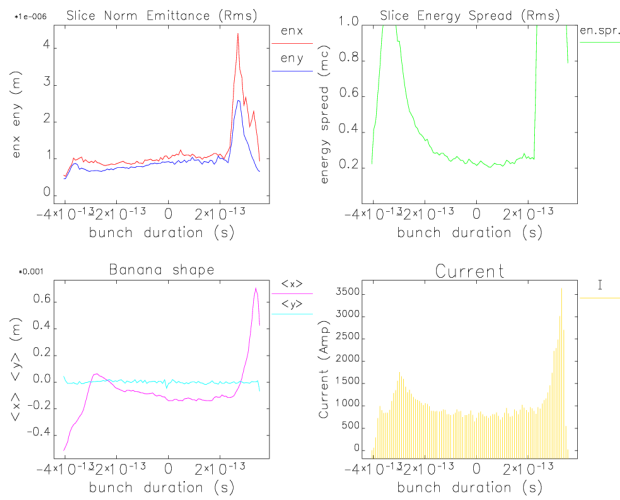


Figure 2: Slice properties of the electron bunch at the exit of BC1 *without* collimation. The bunch head is at the negative time coordinate.

Because of the energy/horizontal position correlation in BC1, the collimator blades placed at both sides of the vacuum chamber are able to stop particles at horizontal coordinate |x|>6mm from the bunch centroid when the beam is passing through the inner drift of BC1. The comparison of Figure 2 and 3 shows that the scraper reduces the total bunch length of the compressed beam from 8ps to 6ps and that the current spikes are removed.

Particle tracking also shows that, if not kept under control, the optics mismatch of the bunch edges propagates up to BC2 with a degrading impact on the projected emittance. Figure 4 demonstrates that the beam scraping in BC1 mitigates the projected emittance growth

#simone.dimitri@elettra.trieste.it

in BC2, without affecting the slice emittance and the charge density in the bunch core.

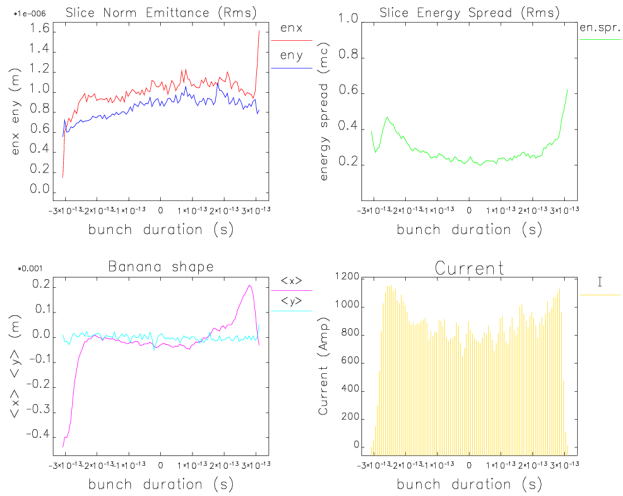


Figure 3: Slice properties of the electron bunch at the exit of BC1 *with* collimation. The bunch head is at the negative time coordinate.

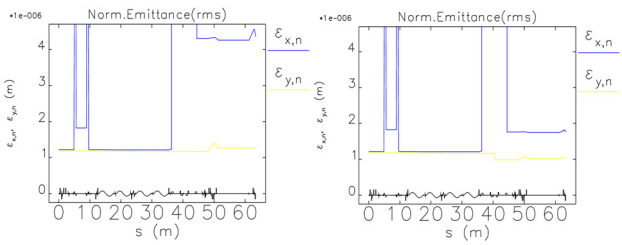


Figure 4: Normalized projected transverse emittances without (left) and with (right) horizontal scraping in BC1.

## *Energy Spread*

Bunch shortening due to the scraper enhances the effect of the geometric longitudinal wake fields in the succeeding accelerating structures. Figure 5 shows the final longitudinal phase space when the scrapers are moved in and out, respectively. The average energy of the unperturbed beam is 1200 MeV, while it is 1205 MeV for the scraped beam. More important, the nominal rms energy spread of the central 0.5ps portion of the bunch is 0.08%. It increases to 0.16% for the scraped beam.

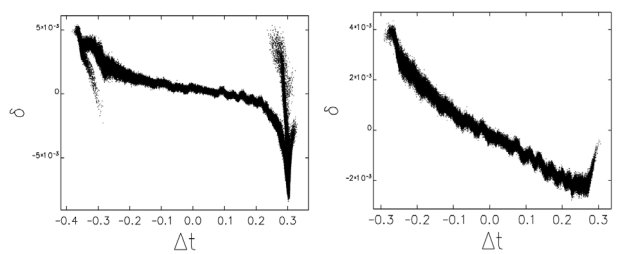


Figure 5: Longitudinal phase space (relative energy spread vs. bunch duration in ps unit) at the entrance of the undulators without (left) and with (right) horizontal scraping in BC1.

To reduce it, a small amount of the linac energy budget must be used to run more off crest the phase of some accelerating structures.

# COLLIMATORS

Geometric Collimators (GC) are cylindrical apertures of reduced diameter [2] located in dispersion-free regions of the lattice. They filter particles in the transverse phase spaces (*x,x'*) and (*y,y'*). Since the FERMI layout was not initially designed having a collimation purpose in mind, the CS has been compressed into a pair of collimators placed downstream of the diagnostic region after BC1 and at the linac end, where a symmetric optics with phase advances of 120deg has been arranged for the multi-screen emittance measurement [9].

In order to minimize the flux of e.m. shower escaping the GCs and to intercept off-energy particles, Energy Collimators (EC) are inserted in the achromats of the FERMI high energy dog-leg. Figure 6 shows the optics from the end of BC1 to the entrance of the undulators. The ECs are in correspondence of the maximum dispersion.

Because the FERMI linac is pulsed, it is conceivable that energy errors will be frequent and will occur at any pulse with no advance notice. On the contrary, all systems that might cause a large betatron oscillation have been designed to be incapable of rapid pulse-to-pulse changes of state. Therefore, it is expected that a bunch with unacceptable betatron oscillations will rarely reach the CS. The EC should be far more resistant to damage from beam power than the geometric collimators.

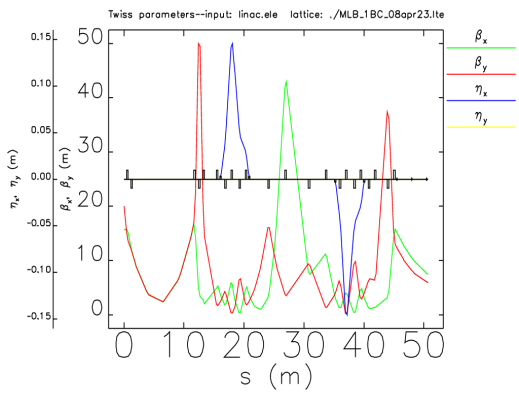


Figure 6: Twiss functions from the end of BC1 (250MeV) to the entrance of the FEL1 undulators (1.2GeV).

## *Geometric Collimation*

The collimation acceptance (defined in the transverse phase space) depends on the collimators gap and on the betatron phase advance between the two collimators [10]. A phase advance $\Delta\mu=\pi/2$ between the collimators and very large betatron functions at the collimators' location maximizes the probability of intercepting a particle having large oscillation amplitudes, since it intercepts both its maximum position and angle. However, a compromise has to be adopted in FERMI between the optics specifications and the available space in the layout.

A definition of collimation efficiency has therefore to be given in order to quantify such a compromise [11].

Simple geometric considerations can be applied to the normalized phase space shown in Figure 7. If $r$ is the collimator half gap onto the phase space, the normalized collimation acceptance is $4r^2/\sin(\Delta\mu)$ for a generic phase advance $\Delta\mu$. The ration between the π/2 acceptance and another θ-acceptance is $a/\tilde{a} = 4r^2/\left(4r^2/\sin\theta\right) = \sin\theta$.

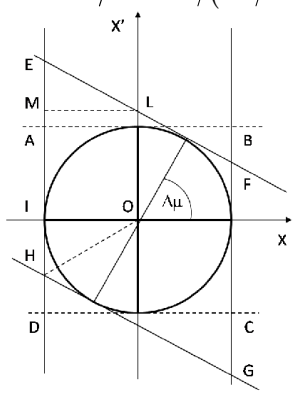


Figure 7: Normalized phase space. If the phase advance between the collimators is not π/2, then the shadow of GCOL1 at the location of GCOL2 is represented by the inclined lines (EF, HG). The new larger acceptance is now the area of the parallelogram EFHG. By geometric considerations we can infer that CG=r/sinθ, FC=r(cosθ/sinθ), BF=r[(1-cosθ)/sinθ]. The ratio between the two acceptances ABCD and EFGH is: $a/\tilde{a} = 4r^2/\left(4r^2/\sin\theta\right) = \sin\theta$.

The clearance Δ between the beam-stay-clear and the inner surface of the undulator vacuum chamber is here arbitrarily fixed at 20% of the undulator beam pipe height $R$. The main goal is therefore to avoid that particles travel through the real space in the ($R$-$r$) region. The actual absorber radius is usually limited by considerations on the transverse wake field perturbation to the regular beam. If $\tilde{r}$ is the actual radius and $r$ is defined by $a_{coll}=r^2/2\beta_{und}$ [9], then we define the collimation efficiency (i.e. the stopping efficiency for unwanted particles) in terms of the absorber radius and of the actual phase advance as follows [11]:

$$\varepsilon_{coll} = \frac{R^2 - \tilde{r}^2}{R^2 - r^2}\sin\left(\Delta\mu_{12}\right) \qquad (1)$$

Figure 8 shows the collimation efficiency and the betatron function at the collimator location as a function of the relative phase advance between the two geometric collimators. Notice that, because of the trigonometric function in (1) and owing to fixed length of the collimator section (~10 m), the maximum collimation efficiency does not necessarily occur at π/2 phase advance. Indeed, for a given collimator gap, a wider phase advance can be accepted if the betatron functions at the collimators become sufficiently large.

Table 1 lists the optics parameters and the collimation efficiency as defined by (1) of the FERMI@elettra GCS.

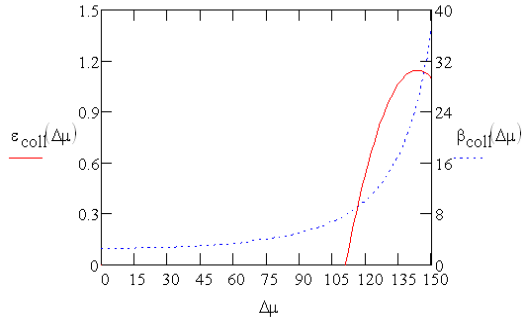


Figure 8: Collimation efficiency and betatron function at the collimator location as a function of the relative phase advance in degrees between the two geometric collimators located in a drift space; the optics is assumed to be symmetric w.r.t. the middle point. The relevant betatron function at the beam waist is 2.5 m; the collimator half gap is 2 mm.

Table 1: Parameters of the GC System.

| | **BC1 Region** | **Linac End** |
|---|---|---|
| β, min. | 3.0m | 2.5m |
| Δμ, max. | 120deg | 120deg |
| Coll.Gap, min. | 2mm | 2mm |
| Coll. Efficiency | 84% | 52% |

### *Energy Collimation*

The dispersion function at the collimator location in each dog-leg achromat is approximately 10 cm. The energy cut is set at ±2% for a collimator radius of 2 mm. The energy acceptance is sufficiently larger than the rms beam energy jitter (0.1%) to ensure that the energy collimators will not intercept the beam core during normal operation. The collimator is set to approximately 18σ from the bunch centroid in the horizontal plane.

## REFERENCES

[1] S. Di Mitri et al., NIM A **608** (2009), 19–27.
[2] S. Ferry et al., WE6RFP043, PAC'09, Vancouver, Canada.
[3] H. Schlarb, "Simulation of dark current transport through the TESLA Test Facility Linac", EPAC'02, Paris, France.
[4] K.L.F. Bane et al., PRST-AB, **8,** 064401 (2005).
[5] J.H. Han et al., PRST-AB, **8,** 033501 (2005).
[6] [G.A. Loew and J. W. Wang, SLAC-PUB-5059 (1989).
[7] Y. Derbenev et al., TESLA-FEL 95-05, 1995.
[8] M. Borland, APS LS-287, 2000.
[9] S. Di Mitri, "Compact Multi-Purpose Optics Insertion in the FERMI@elettra Linac Bunch Compressor Area", Proc. of this Conference.
[10]T. Kamps, "Collimation system for the Bessy FEL", FEL'04, Trieste, Italy.
[11]S. Di Mitri, PRST-AB, **13,** 052801 (2010).